HHS Public Access

Author manuscript

Adv Healthc Mater. Author manuscript; available in PMC 2018 May 01.

Published in final edited form as:

Adv Healthc Mater. 2017 May ; 6(10): . doi:10.1002/adhm.201601333.

Aligned Nanofibrous Cell-Derived Extracellular Matrix for Anisotropic Vascular Graft Construction

Qi Xing, **Zichen Qian**, **Mitchell Tahtinen**, **Ai Hui Yap**, **Keegan Yates**, and **Feng Zhao***

Department of Biomedical Engineering, Michigan Technological University, 1400 Townsend Drive, Houghton, MI 49931, U.S

Abstract

There is a large demand for tissue engineered vascular grafts for the application of vascular reconstruction surgery or *in vitro* drug screening tissue model. The extracellular matrix (ECM) composition, along with the structural and mechanical anisotropy of native blood vessels are critical to their functional performance. The objective of this study was to develop a biomimetic vascular graft recapitulating the anisotropic features of native blood vessels by employing nanofibrous aligned fibroblast-derived ECM and human mesenchymal stem cells (hMSCs). The nanotopographic cues of aligned ECM directed the initial cell orientation The subsequent maturation under circumferential stress generated by a rotating wall vessel (RWV) bioreactor further promoted anisotropic structural and mechanical properties in the graft. The circumferential tensile strength was significantly higher than longitudinal strength in bioreactor samples. Expression of smooth muscle cell specific genes, α-smooth muscle actin and calponin, in hMSCs was greatly enhanced in bioreactor samples without any biochemical stimulation. In addition, employment of pre-made ECM and RWV bioreactor significantly reduced the graft fabrication time to 3 weeks. Mimicking the ECM composition, cell phenotype, structural and mechanical anisotropy, the vascular graft presented in our study is promising for vascular reconstruction surgery or *in vitro* tissue model applications.

Keywords

anisotropic vascular graft; extracellular matrix nanofibers; human mesenchymal stem cells; myogenic phenotype; rotating wall vessel bioreactor

1. Introduction

Vascular grafts for coronary and peripheral bypass surgery are in large demands due to the high occurrence of cardiovascular diseases. An emerging trend of using engineered living tissues for drug screening purposes also requires functional artificial vessels as one of the model systems [1]. A completely biological tissue-engineered vascular graft composed of extracellular matrix (ECM) with living cells is promising for both applications as it effectively mimics the components, mechanical strength, and physiological functions of

Corresponding to: Feng Zhao, Department of Biomedical Engineering, Michigan Technological University, 1400 Townsend Drive, Houghton, MI 49931, U.S., Tel: 906-487-2852, Fax: 906-487-1717, fengzhao@mtu.edu.

native blood vessels. The stromal environment of native blood vessels is composed of ECM fibers at the nano- and micro-scale which provide mechanical support for vascular cells [2]. The ECM also acts as a reservoir of growth factors and cytokines that regulate cell attachment, migration, proliferation, and physiological response. These proper cellular activities are closely associated with remodeling and regeneration of blood vessels [3]. In addition, the specific ECM and cell organization in native blood vessels give rise to anisotropic characteristics that are critical to their mechanical and functional performance. The circumferentially aligned ECM fibers and smooth muscle cells (SMCs) in the tunica media are crucial to regulate vasoconstriction, vasodilation, as well as the mechanical anisotropy of blood vessels [4]. Matching mechanical properties to host vessels is also important for determining vascular graft patency rates and maintaining the endothelium phenotype [5]. Thus, replication of the ECM composition as well as structural and mechanical anisotropy of native vessels in engineered vascular grafts may improve *in vivo* tissue regeneration or maintain vessel function *in vitro*.

Cell-derived ECM provides an alternate option to native tissue-derived ECM for engineering completely biological vascular grafts. Cell-derived ECM contains a complex mixture of ECM molecules including collagen, elastin, and proteoglycans that are found in native vessels. Compared to tissue-derived matrices, cell-derived ECM is more versatile in customization by selecting different cell sources, culture methods, and external stimulation such as topographical cues and mechanical conditioning. Several groups reported using fibroblast-derived ECM for vascular graft fabrication. The earliest tempt was using self-assembly technique by wrapping fibroblast cell sheets around a temporary mandrel into tubular grafts followed by devitalization. The acellular graft was seeded with autologous endothelial cells (ECs) inside the lumen achieving an autologous graft which remained to be patent after 8 weeks post implantation for hemodialysis access [6]. Another group using the same technique but decellularized the fibroblast cell sheet to obtain ECM, seeded autologous SMCs, and then rolled up to form tubular constructs [7]. These two studies demonstrated the feasibility of fabricating vascular grafts based on fibroblast-derived ECM and its clinical application potential; however, no anisotropic features were characterized. Culturing fibroblasts in a sacrificial tubular fibrin gel mold under pulsatile flow resulted in an arterial graft with circumferential alignment and mechanical anisotropy similar to native arteries [8]. The *in vivo* implantation of the decellularized graft demonstrated complete endothelialization, significant mature SMCs invasion, as well as substantial ECM deposition and remodeling [9]. However, the graft manufacturing time is relatively long, taking about 5 weeks. Highly mimicking the anisotropic structure while dramatically shortening the fabrication time could significantly amplify the function and clinical application of the engineered vascular grafts.

We have previously developed a highly aligned fibroblast cell sheet derived ECM using nanograted substrates. It contains parallel lined ECM fibers with diameter around 80 nm, which is close to the dimension of collagen fibrils found in human body. The aligned ECM supported the proliferation of human mesenchymal stem cells (hMSCs) and directed the cellular orientation through contact guidance [10]. Additionally, the *in vitro* macrophages secreted less pro-inflammatory cytokines when cultured on aligned ECM. Previous studies have demonstrated that fibroblast-derived ECM is a suitable material for vascular graft

fabrication because it provides sufficient mechanical strength and allows for host cell penetration and remodeling. Employment of aligned fibroblast-derived ECM can create anisotropic features, which better mimic the structural characteristics of native vessels. hMSCs can serve as an alternative cell source for vascular grafts due to the fact that they are antithrombogenic, immunoregulatory, and can be differentiated into vascular cells. [1, 11]. Rotating wall vessel (RWV) bioreactor, a relatively simple dynamic culture system, provides not only efficient exchange of nutrients and wastes, but also mechanical conditioning in circumferential direction. Although the RWV bioreactor has been employed to improve biological or mechanical performance of 3D constructs [12], its application in generating anisotropic features in tissue constructs is rarely reported.

In this work, we employed the aligned nanofibrous ECM and hMSCs to fabricate an anisotropic vascular graft within 3 weeks under the stimulation of circumferential stress generated in a RWV bioreactor. The graft in bioreactor showed significantly enhanced structural and mechanical anisotropy. In addition, the bioreactor samples displayed more uniform cell distribution and increased SMC phenotype expression. The structural and mechanical resemblances to native blood vessels make this anisotropic graft a promising candidate for vascular reconstruction surgery or *in vitro* drug screening models. The relatively short tissue culture period also simplified the handling process and facilitated future clinical applications.

2. Results

Fabrication of 3D anisotropic tissue construct

The procedure for 3D anisotropic tissue construct fabrication is illustrated in Figure 1. Briefly, human dermal fibroblasts were seeded on top of a nanograted polydimethylsiloxane (PDMS) substrate and allowed to grow 6 weeks to form a thick and highly aligned cell sheet. After decellularization, the resulting ECM maintained the anisotropic structure [10]. The average pore area is 0.07 ± 0.01 μm^2, and the fraction of total pore area is around 50.1 ± 6.1%. The thickness of the ECM is around 35 μm. Before being seeded with hMSCs, the ECM can be stored in −80 °C freezer for future use. The hMSCs grown on the aligned ECM oriented along the ECM nanofibers. When cells became confluent, the tissue sheets were rolled around a stainless steel cylinder-shaped mandrel (diameter: 2 cm) to form tubular constructs. The constructs with the mandrel were put in RWV bioreactors and cultured for 2 weeks at low speed (5 rpm) or high speed (20 rpm). Rotating wall vessel bioreactor rotates horizontally and counter-clockwise, generating shear stress in the circumferential direction exerting on the constructs sitting at the bottom of bioreactor. The mechanical stress experienced by the constructs during the dynamic culture was estimated to be around 3.02 Pa (5 rpm) and 8.95 Pa (20 rpm). The construct without mechanical stimulation was employed as static control. Finally the tubular construct was carefully removed from the mandrel and used for analysis.

Morphology observation and cell distribution of the tissue construct

The SEM images in Figure 2 demonstrate that the external and internal surfaces of the 3D constructs from bioreactor culture were quite different than those from static culture. On the

external surfaces of the bioreactor samples, parallel grooves were clearly observed in the direction of circumferential stress, while static sample surfaces were much smoother. High magnification images revealed the ultrastructure of external surfaces. The static sample surfaces were composed of numerous ECM nanofibers; whereas, the nanofibers in bioreactor samples fused into thick ECM bundles. For all samples, cells could be observed on the internal surfaces of the constructs. In addition, the cells showed preferred alignment on bioreactor samples compared to static samples. The cell distribution was examined by nucleus and F-actin staining of the cross section of tubular constructs (Figure 2). All samples demonstrated multiple concentric layers of cells and F-actin stress fibers. The thickness of the construct wall was estimated as 166.7 ± 22 μm, 208.3 ± 18 μm, 250.4 ± 11 μm for static, 5 rpm, and 20 rpm samples, respectively. In the static samples, there were more cells and F-actin fibers found in the outermost layers than in the inner layers. In bioreactor samples, the cell distribution was more uniform throughout the layers. The 20 rpm samples had the most intensive expression of F-actin in the outermost layer indicating thicker and denser stress fiber formation.

ECM structure and content in the tissue construct

In order to examine the ECM structure inside the wall of the 3D constructs, ECM proteins including collagen I, III, and IV, as well as fibronectin and elastin were stained (Figure 3 A). All samples showed positive staining for these ECM proteins with highly aligned ECM fibers. Compared to the static control, the bioreactor samples demonstrated slightly thicker ECM fibers, especially structural proteins collagen I and elastin. The quantitative analysis of ECM contents demonstrated that the mechanical stimulation decreased the collagen production, but increased glycosaminoglycans (GAGs) content when the rotating speed was increased (Figure 3B). The average collagen amount per mg wet tissue decreased around 26.8% ($p < 0.05$), and the average GAGs increased around 32.9% ($p < 0.05$) from static cultures to 20 rpm dynamic cultures. The elastin content was not significantly influenced by the mechanical stimulation.

Anisotropic mechanical strength of the tissue construct

The stress-strain response of the engineered tissue is non-linear, as observed in many native tissues [4]. Uniaxial tensile testing was performed along longitudinal and circumferential directions to evaluate the mechanical strength of the 3D tissue constructs (Figure 4). In the longitudinal direction, the average ultimate tensile stress (UTS) of 5 and 20 rpm samples decreased around 55% and 75%, respectively, compared to the static samples. The corresponding modulus of bioreactor samples was also significantly lower than the static samples ($p < 0.05$). However, there was no significant difference for ultimate strain among all three samples ($p > 0.05$). In the circumferential direction, the average UTS of 5 rpm and 20 rpm samples increased around 48% and 90%, respectively, compared to the static samples. No significant difference was found between 5 rpm and 20 rpm samples ($p > 0.05$). Correspondently, the elastic modulus of bioreactor samples was significantly higher than the static samples ($p < 0.01$). The ultimate strain in the circumferential direction was also comparable among bioreactor and static samples ($p > 0.05$). These results demonstrated that the mechanical stimulation exerted in the circumferential direction significantly increased the tensile strength of the tissue measured in the same direction, but decreased the tensile

strength measured in the longitudinal direction. All samples exhibited anisotropic mechanical properties. The UTS measured in circumferential direction was significantly higher than that measured in longitudinal direction for bioreactor samples ($p < 0.01$). The moduli of bioreactor samples were also much higher in the circumferential direction ($p < 0.01$). On the opposite, the longitudinal UTS and moduli were higher than the circumferential counterparts for static samples. In addition, the ultimate strain was greater in the longitudinal direction for bioreactor samples. The average circumferential to longitudinal UTS ratio (anisotropy index) was around 0.46 ± 0.01, 1.50 ± 0.13, and 3.22 ± 1.21 for static, 5 rpm and 20 rpm, respectively.

Myogenic phenotype expression in the tissue construct

The SMC-specific phenotype expression of the engineered anisotropic hMSC construct was examined. The expression of myogenic genes including α-smooth muscle actin (α-SMA), calponin, and smooth muscle myosin heavy chain (SM-MHC) from hMSC constructs in different cultures is demonstrated in Figure 5. The gene expression of hMSC constructs cultured in complete culture medium was normalized to static samples (Figure 5 A). Myogenic genes were significantly enhanced in bioreactor samples, compared to static samples, without any extra biochemical induction ($p < 0.01$): α-SMA (around 3 and 4 fold increases for 5 rpm and 20 rpm samples, respectively), calponin (around 2 fold increase for both 5 rpm and 20 rpm samples); whereas SM-MHC expression did not change significantly ($p > 0.05$). The immunofluorescence staining also confirmed that α-SMA, and calponin intensity was higher in bioreactor samples than in static samples (Figure 5 C). The gene expression of hMSC constructs cultured in smooth muscle induction medium was normalized to the corresponding static control (Figure 5 B). The α-SMA and calponin expression in bioreactor samples was much higher than in static samples ($p < 0.01$). On the contrary, the SM-MHC expression in static samples was around 60 times higher than in bioreactor samples.

Discussion

An engineered vascular graft with features resembling the composition, anisotropic structure and mechanical strength of native blood vessels is critical for improving *in vivo* tissue regeneration and recapitulating *in vitro* tissue performance. In our study, fibroblast-derived aligned nanofibrous ECM was employed for vascular graft fabrication, as it can provide suitable compositional, structural, and mechanical cues using proper manufacturing methods. In addition, the ECM can be produced and stored in advance, which helps to reduce graft maturation time by 1–2 weeks compared to previously published approaches for fabricating completely biological grafts [13]. Application of RWV bioreactor further promoted anisotropic features and SMC phenotype expression in hMSCs.

Circumferential stress promotes structural and mechanical anisotropy

The cell and ECM organization of the hMSC constructs in bioreactor culture demonstrated strong anisotropic structure. During the dynamic culture, the constructs experienced high mechanical stress of 3.02 Pa (5 rpm) and 8.95 Pa (20 rpm) in circumferential direction, which may be responsible for inducing tissue contraction and formation of thick ECM fiber

bundles aligned in the same direction (Figure 2). The similar phenomenon was also observed in another study which reported the appearance of larger collagen fibrils and tissue contraction in fibroblast-derived cell sheets experiencing circumferential cyclic stretch [14]. The formation of circumferentially aligned structure may induce rapid regeneration of tunica media *in vivo* [15]. Alignment also has potential anti-inflammatory effects by reducing circulating monocytes adhesion to endothelium [16]. The more uniform cell distribution in bioreactor samples indicated that the bioreactor might provide better nutrient infiltration throughout the multilayer structure. The F-actin stress fibers, in response to mechanical stresses, became thicker and denser. It has been reported that aligned or thicker stress fibers result in reinforced cell stiffness [17] which is closely associated with cell status. Collagen and elastic fibers are the two most important ECM components that endow the natural tissues critical mechanical properties such as flexibility and extensibility [18]. The bioreactor culture did not increase the amount of deposited collagen and elastin as shown in Figure 3 B, the mechanical properties difference between static and bioreactor samples (Figure 4) were more likely determined by the structure of the constructs.

The bioreactor samples demonstrated strong mechanical anisotropy – UTS measured in the circumferential direction was around 48% to 90% higher than those measured in the longitudinal direction. This mechanical strength discrepancy was mainly determined by structure difference. Under the continuous circumferential mechanical stress stimulation, the cell and ECM fibers in bioreactor samples were primarily aligned in the circumferential direction and the tissue constructs contracted in the longitudinal direction, which led to much higher strength in the aligned direction as reported in other studies [19]. Native vessels demonstrate directional dependent mechanical strength. For example, the tensile strength of healthy human ascending thoracic aortic wall in the circumferential direction is much higher than in the longitudinal direction (1.20 ± 0.20 vs. 0.66 ± 0.07 MPa) [20]. Our findings of 0.28 – 1.19 MPa UTS for the hMSC construct was at the same magnitude and close to the mechanical strength for native muscles. The anisotropy index of 1.50 to 3.22 for bioreactor samples was also comparable to that of native vessels (1.8 for human ascending aorta and 3.4 for ovine femoral artery) [13b]. The matching of mechanical properties to native tissue may facilitate the restoration of mechanical and biological functions when integrated into native tissue. On the contrary, the static sample showed much higher UTS in the longitudinal than in the circumferential direction. When assembled on a tubular mandrel, the tissue sheets tended to stretch along the mandrel longitudinally which may contribute to the directional discrepancy in static samples. In addition, the circumferential UTS and modulus of bioreactor samples were significantly higher than those of static samples. This phenomenon was possibly due to the effect of circumferentially aligned thick ECM fiber bundles and stress fibers in bioreactor samples.

Circumferential stress promotes myogenic phenotype expression

The differentiation of hMSCs into SMCs using biochemical or mechanical stimulation has been reported by different groups; however, most of the studies performed the myogenic differentiation in conventional 2D cell culture plates (ECM protein coated or untreated) [21]. A few publications reported the myogenic differentiation of hMSCs in simple 3D scaffolds such as silicon tube, polyglycolic acid mesh, or poly-L-lactic acid nanofibrous

scaffold [11b, 22]. The combination of complex ECM microenvironment, 3D structure, and dynamic culture may create a more physiological relevant system. In our study, the mechanical stress generated in a bioreactor alone significantly enhanced the gene expression of α-SMA and calponin (early SMC contractile phenotype proteins). This is consistent with previous studies that mechanical stimulation can increase myogenic protein expression of hMSCs *in vitro* [11b, 21a]. However, the simultaneous stimulation of mechanical stress and myogenic induction medium significantly decreased myogenic gene – SM-MHC expression. A similar phenomenon was also observed in another study which showed that hMSCs induced by cyclic strain plus platelet derived growth factors had less myogenic protein expression than those induced by a single factor [11b]. Phenotype transition towards a contractile state is required for SMCs to perform their contraction and dilation function [23]. These evidences suggest that the hMSCs in our dynamic cultured constructs possess the potential to differentiate towards SMCs without extra biochemical induction.

Several studies have successfully employed the similar approach of rolling “cell sheets” (including fibroblast, SMC, and hMSC sheets) to form vascular grafts [1, 7, 13a]. These grafts are completely biological and exhibit suitable mechanical strength or vasodilation characteristics. Compared to other studies, our anisotropic grafts combined the following advantages: first, the circumferentially aligned ECM and anisotropic mechanical property of the tubular constructs resemble the structure and strength of native arterial wall. Second, the hMSCs in the constructs expressed strong SMC contractile phenotypes at both gene and protein levels that indicated the possibility to perform normal functions as SMCs. Third, The ready-to-use cell-derived ECM significantly shortened tissue culture time. Fourth, the increased intensive staining of connexin 43 in bioreactor samples (Supplementary Figure 1) indicated stronger cell-cell communication, which may contribute to regulate the elasticity of the vascular wall [26]. In this study, we assumed a strictly circumferential SMC orientation in vascular grafts; whereas, in natural blood vessels, the SMC orientation shows considerable dispersion predominantly in the helical direction [27]. This orientation pattern could be realized by wrapping the cell sheets around the mandrel with certain angles. The property dependence of the engineered vascular grafts on the orientation angles of SMCs will be our future research goal.

Conclusions

In conclusion, we utilized aligned nanofibrous fibroblast ECM in combination of RWV bioreactor to generate a vascular graft with physiological orientation and mechanical strength. The graft consisted of multiple layers of tissue sheets exhibiting highly aligned thick ECM fiber bundles on the surface and uniformly distributed cells throughout the construct. The application of circumferential stress to the construct significantly increased the tensile strength in the same direction and enhanced the degree of anisotropy compared to static samples. The mechanical stimulation also enhanced the expression of early myogenic markers α-SMA and calponin from hMSCs without biochemical induction. The highly organized cellular and ECM architecture, anisotropic mechanical strength, and SMC phenotype expression enabled the graft to be a promising approach for vascular reconstruction surgery or *in vitro* drug screening model.

Methods

Fabrication of natural ECM scaffold

The ECM scaffold was obtained using our previously published method [28]. Briefly, the nano-patterned (130 nm in depth, 350 nm in groove width, and 700 nm in period) PDMS was coated with bovine collagen I to facilitate cell adhesion. Human dermal fibroblasts (ATCC, Manassas, VA) at the passage from 3 to 5 were seeded on the PDMS at a density of 10,000 cells/cm^2. The cells were cultured in Dulbecco's Modified Eagle Medium (DMEM) supplemented with 20% fetal bovine serum (FBS), 20% Ham F12, 500 μM sodium ascorbate, and 1% penicillin/streptomycin. After 6 weeks, the resulting cell sheet was first placed into the decellularization solution containing 1 M NaCl, 10 mM Tris, and 5 mM EDTA (Sigma, St Louis, MO) and shaken for 1 h at room temperature. After thoroughly rinsed with phosphate buffered saline (PBS), the cell sheet was then placed in a second decellularization solution containing 0.5 % SDS, 10 mM Tris, and 5 mM EDTA (Sigma), and shaken for 0.5 h at room temperature. After a PBS wash, the sample was rinsed in DMEM medium with 20% FBS for 48 h at room temperature and rinsed again with PBS. The thickness of the ECM scaffold was examined by scanning fluorescence staining of collagen I in ECM under 488 nm laser excitation using an Olympus FV-1000 confocal microscope (Olympus America, Center Valley, PA). The average pore area and pore area fraction were assessed by analyzing SEM images of ECM scaffolds using ImageJ as previously described [29]. The automated threshold was set on enhanced SEM image. The highlighted part was measured as fiber area and the dark area was measured as pore area. Six different views were randomly chosen for analysis.

Fabrication of ECM-hMSC vascular grafts

The hMSCs were seeded on the ECM scaffold (6 cm × 4 cm) at the density of 10,000 cells/cm^2 and cultured in complete culture medium: alpha-MEM supplemented with 20% FBS, 1% L-glutamine, and 1% penicillin/streptomycin (Life Technologies, Rockville, MD). After 7 days, two tissue sheets were rolled around a tubular stainless steel mandrel (diameter: 2 mm; length: 9 cm) to form tubular constructs, which were further cultured in the same medium for 14 days either in a RWV bioreactor (Synthecon, Houston, TX) at 5 rpm and 20 rpm or in static condition.

Morphology observation

Tubular constructs were carefully removed from the mandrel and opened up with scissors along the central line. Samples were fixed with 4% formaldehyde, washed with PBS, and then dehydrated through a graded series of ethanol/PBS solutions. Finally the samples were dried in Hexamethyldisilazane (Sigma) and viewed using a Hitachi S-4700 field emission scanning electron microscope. Standard histological stains of hematoxylin & eosin (HE) was performed on cryosection of vascular graft cross section.

ECM characterization and immunofluorescent staining

The expression of the ECM proteins collagen I, III, IV, fibronectin, and elastin were examined by immunofluorescent staining following our previous publication [28]. The

tubular constructs were opened up along the longitudinal direction. Samples were fixed, blocked, and incubated with the primary antibodies (Abcam, Cambridge, MA). After being washed, samples were incubated with secondary antibody conjugated to Alexa Fluor 488. Then the samples were mounted and viewed using an Olympus FV-1000 confocal microscope. Collagen content was quantified by a colorimetric analysis using a hydroxyproline assay kit as previously described, assuming collagen to hydroxyproline ratio is 10:1 w/w [28]. Elastin content was quantified using the Fasting Elastin Assay Kit as previously described [28]. The GAG content of the tubular constructs was determined using the Blyscan Sulfated GAG Assay Kit (Biocolor, United Kingdom) following our previously published method [28].

Mechanical strength test

In order to characterize the uniaxial tensile strength of the tubular tissue construct, the tubes were opened up along the center line and cut into rectangular strips with dimension of 6 mm × 12 mm in both longitudinal and circumferential directions. The thickness of the construct wall was estimated by measuring the thickness of collagen I fluorescence staining in cross section of the tubular constructs. The specimens were fixed to the grips (sandpaper was attached to prevent slipping) of a dynamic mechanical analyzer (DMA Q800). The pulling force was controlled at 0.5 N/min. The UTS and the ultimate strain were defined as the maximum stress and strain recorded before the sample failure. The elastic modulus was defined as the slope of the linear portion of the stress-strain curve.

Myogenic induction

The 3D tubular constructs were cultured in smooth muscle myogenic induction medium or complete culture medium under static or dynamic conditions for two weeks. The formulation of myogenic induction medium was adopted from previous publications [21b, 30]. The smooth muscle myogenic medium consisted of α-MEM, 1 ng/mL TGF-β1, 30 μM ascorbic acid, and 20% FBS. The samples cultured in complete culture medium were used as control.

Myogenic gene analysis

After 14 days of culture in induction medium or control medium, total RNA from different cultures were isolated using the RNeasy Mini kit (Qiagen, Valencia, CA). Reverse transcription (RT) was performed using 8 pg of total RNA with RT reaction mixture, which contains primers specific for target genes that were purchased from sigma and normalized to GAPDH as an endogenous control. The myogenic genes including α-SMA, calponin, SM-MHC were examined. Reverse transcription-polymerase chain reaction (RT-PCR) reactions were performed on StepOnePlus RT-PCR system (Applied Biosystems, Foster City, CA), using SYBR1 Green PCR Master Mix. The amplification reactions were carried out for up to 40 cycles. Fold variation in gene expression was quantified using the comparative Ct method: $2^{-\Delta(\Delta CtTreatment-\Delta CtControl)}$.

Estimation of mechanical stress exerted on the 3D construct

The RWV bioreactor was filled with 250 mL of the complete hMSC culture medium, which occupied only half volume of the rotating vessel. The tubular tissue stayed at the bottom of the vessel due to the weight of the stainless steel mandrel. The flow pattern in the vessel is quite different from that in the conventional RWV bioreactor. The medium flow was brought up to the liquid surface and circulated down back into the bulk medium. The flow field in the bioreactor cannot be simplified as a laminar flow condition. The average mechanical stress exerted on the tubular tissue can be estimated by force balance analysis and calculated by the following equation:

$$\tau_e = \frac{F}{A} = \frac{(m_m + m_t + m_i)\, g \sin\theta}{A}$$

τ_e is the effective stress applied on the construct; F is the force applied to the construct on the mandrel; F drives the construct stray away from the vertical line of the bioreactor and is counterbalanced by gravity of the mandrel with the tubular tissue; m_m is the mass of the mandrel (approximately 1.0 g); m_t is the mass of the tissue construct (approximately 0.13 g); m_j is the mass of the medium filling inside of the mandrel (approximately 0.28 g); g is the gravity acceleration; θ is the angle between construct position and vertical line of bioreactor; A is the cross section area where the force applied. A is approximated as the longitudinal cross section area of the mandrel (length: 9 cm; outer diameter: 2 mm).

Statistics/data analysis

Experiment results were expressed as means ± standard deviation (SD) of the means of the samples. For each set of experiment, at least three samples were investigated. Student's t-test (Microsoft Excel) was used for comparisons and statistical significance was accepted at $p < 0.05$.

Supplementary Material

Refer to Web version on PubMed Central for supplementary material.

Acknowledgments

This study was supported by the National Institutes of Health (1R15CA202656 and 1R15HL115521-01A1) and the Research Excellence Fund-Research Seed Grant (REF-RS) from Michigan Technological University. The authors wish to thank Dr. Jeffrey Allen in the Department of Mechanical Engineering at Michigan Technological University for his help in mechanical stress analysis and Dr. Yu Zhao in our research group for his help in drawing graphic illustration of the 3D tissue construct fabrication process (Figure 1).

References

1. Jung Y, Ji HY, Chen ZZ, Chan HF, Atchison L, Klitzman B, Truskey G, Leong KW. Sci Rep. 2015; 5:15116. [PubMed: 26456074]
2. Stehbens WE, Martin BJ. Connect Tissue Res. 1993; 29:319. [PubMed: 8269707]
3. Thottappillil N, Nair PD. Vascular Health and Risk Management. 2015; 11:79. [PubMed: 25632236]
4. Zhou J, Fung YC. Proc Natl Acad Sci U S A. 1997; 94:14255. [PubMed: 9405599]

5. a) Kidson IG. Ann R Coll Surg Engl. 1983; 65:24. [PubMed: 6218775] b) Lee JM, Wilson GJ. Biomaterials. 1986; 7:423. [PubMed: 2947639]
6. Wystrychowski W, Cierpka L, Zagalski K, Garrido S, Dusserre N, Radochonski S, McAllister TN, L'Heureux N. J Vasc Access. 2011; 12:67. [PubMed: 21360466]
7. Bourget JM, Gauvin R, Larouche D, Lavoie A, Labbe R, Auger FA, Germain L. Biomaterials. 2012; 33:9205. [PubMed: 23031531]
8. Syedain ZH, Meier LA, Lahti MT, Johnson SL, Tranquillo RT. Tissue Eng Part A. 2014; 20:1726. [PubMed: 24417686]
9. Syedain Z, Reimer J, Lahti M, Berry J, Johnson S, Tranquillo RT. Nat Commun. 2016; 7:12951. [PubMed: 27676438]
10. Xing Q, Vogt C, Leong KW, Zhao F. Adv Funct Mater. 2014; 24:3027. [PubMed: 25484849]
11. a) Hashi CK, Zhu YQ, Yang GY, Young WL, Hsiao BS, Wang K, Chu B, Li S. Proc Natl Acad Sci U S A. 2007; 104:11915. [PubMed: 17615237] b) Gong ZD, Niklason LE. FASEB J. 2008; 22:1635. [PubMed: 18199698] c) Jorgensen C, Gordeladze J, Noel D. Curr Opin Biotechnol. 2004; 15:406. [PubMed: 15464369] d) Ghannam S, Bouffi C, Djouad F, Jorgensen C, Noel D. Stem Cell Res Ther. 2010; 1:2. [PubMed: 20504283]
12. a) Song KD, Liu TQ, Cui ZF, Li XQ, Ma XH. J Biomed Mater Res A. 2008; 86A:323.b) Arrigoni C, Chitto A, Mantero S, Remuzzi A. Biotechnol Bioeng. 2008; 100:988. [PubMed: 18383121]
13. a) L'Heureux N, Paquet S, Labbe R, Germain L, Auger FA. FASEB J. 1998; 12:47. [PubMed: 9438410] b) Syedain ZH, Meier LA, Bjork JW, Lee A, Tranquillo RT. Biomaterials. 2011; 32:714. [PubMed: 20934214] c) Quint C, Kondo Y, Manson RJ, Lawson JH, Dardik A, Niklason LE. Proc Natl Acad Sci U S A. 2011; 108:9214. [PubMed: 21571635]
14. Weidenhamer NK, Tranquillo RT. Tissue Eng Part C Methods. 2013; 19:386. [PubMed: 23126441]
15. Zhu M, Wang Z, Zhang J, Wang L, Yang X, Chen J, Fan G, Ji S, Xing C, Wang K, Zhao Q, Zhu Y, Kong D, Wang L. Biomaterials. 2015; 61:85. [PubMed: 26001073]
16. Nakayama KH, Joshi PA, Lai ES, Gujar P, Joubert LM, Chen B, Huang NF. Regen Med. 2015; 10:745. [PubMed: 26440211]
17. Gavara N, Chadwick RS. Biomechanics and Modeling in Mechanobiology. 2016; 15:511. [PubMed: 26206449]
18. Lu QJ, Ganesan K, Simionescu DT, Vyavahare NR. Biomaterials. 2004; 25:5227. [PubMed: 15110474]
19. a) Isenberg BC, Backman DE, Kinahan ME, Jesudason R, Suki B, Stone PJ, Davis EC, Wong JY. J Biomech. 2012; 45:756. [PubMed: 22177672] b) Zou Y, Zhang Y. Ann Biomed Eng. 2009; 37:1572. [PubMed: 19484387]
20. Garcia-Herrera CM, Atienza JM, Rojo FJ, Claes E, Guinea GV, Celentano DJ, Garcia-Montero C, Burgos RL. Med Biol Eng Comput. 2012; 50:559. [PubMed: 22391945]
21. a) Kobayashi N, Yasu T, Ueba H, Sata M, Hashimoto S, Kuroki M, Saito M, Kawakami M. Exp Hematol. 2004; 32:1238. [PubMed: 15588948] b) Narita Y, Yamawaki A, Kagami H, Ueda M, Ueda Y. Cell Tissue Res. 2008; 333:449. [PubMed: 18607632] c) Suzuki S, Narita Y, Yamawaki A, Murase Y, Satake M, Mutsuga M, Okamoto H, Kagami H, Ueda M, Ueda Y. Cells Tissues Organs. 2010; 191:269. [PubMed: 19940434]
22. a) Tian H, Bharadwaj S, Liu Y, Ma H, Ma PX, Atala A, Zhang Y. Biomaterials. 2010; 31:870. [PubMed: 19853294] b) Kim D, Heo SJ, Kim SH, Shin J, Park S, Shin JW. Biotechnol Lett. 2011; 33:2351. [PubMed: 21805363]
23. Fisher SA. Physiol Genomics. 2010; 42A:169. [PubMed: 20736412]
24. Zhao F, Veldhuis JJ, Duan YJ, Yang Y, Christoforou N, Ma T, Leong KW. Mol Ther. 2010; 18:1010. [PubMed: 20179678]
25. Xing Q, Qian Z, Kannan B, Tahtinen M, Zhao F. ACS Appl Mater Interfaces. 2015; 7:23239. [PubMed: 26419888]
26. Haefliger JA, Nicod P, Meda P. Cardiovascular Research. 2004; 62:345. [PubMed: 15094354]
27. Spronck B, Megens RTA, Reesink KD, Delhaas T. Biomechanics and Modeling in Mechanobiology. 2016; 15:419. [PubMed: 26174758]

28. Xing Q, Yates K, Tahtinen M, Shearier E, Qian ZC, Zhao F. Tissue Eng Part C Methods. 2015; 21:77. [PubMed: 24866751]
29. Ju YM, Choi JS, Atala A, Yoo JJ, Lee SJ. Biomaterials. 2010; 31:4313. [PubMed: 20188414]
30. Gang EJ, Jeong JA, Hong SH, Hwang SH, Kim SW, Yang IH, Ahn C, Han H, Kim H. Stem Cells. 2004; 22:617. [PubMed: 15277707]
31. Xing Q, Zhao F, Chen S, McNamara J, DeCoster MA, Lvov YM. Acta Biomater. 2010; 6:2132. [PubMed: 20035906]
32. Zhao F, Grayson WL, Ma T, Bunnell B, Lu WW. Biomaterials. 2006; 27:1859. [PubMed: 16225916]
33. Kim J, Ma T. J Cell Biochem. 2013; 114:716. [PubMed: 23060043]

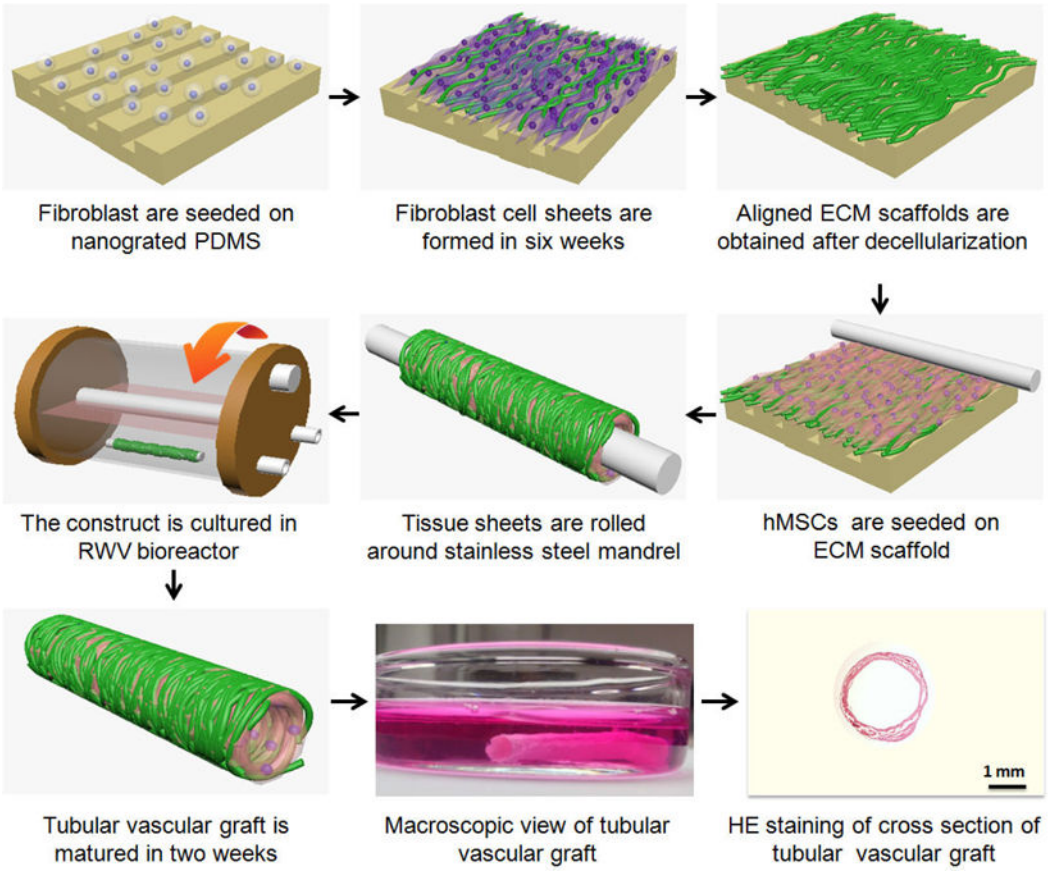

Figure 1.

Schematic illustration of the vascular grafts fabrication process. Highly aligned ECM scaffold was obtained by decellularization of a thick fibroblast cell sheet grown on a nanograted PDMS substrate. The hMSCs-repopulated sheet was rolled around a mandrel and then cultured in either a RWV bioreactor or the static condition for two weeks. The mandrel was removed to form a mature tubular construct. The macroscopic image of engineered tubular vascular graft and HE staining of graft cross section were shown.

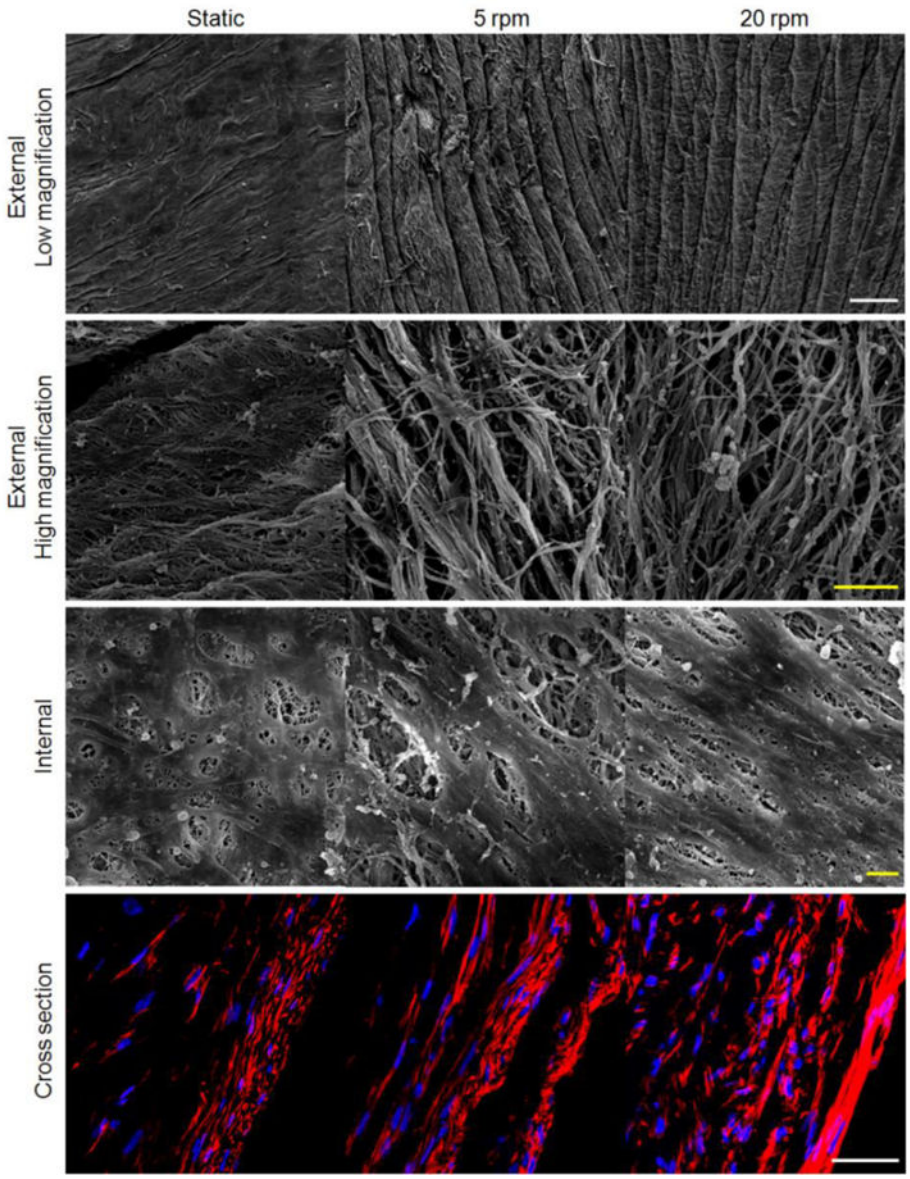

Figure 2.

Morphology of the external and internal surface as well as cross section of the vascular grafts. The external surface of bioreactor samples showed parallel grooves that were not seen on static samples. Thick ECM bundles formed by nanofibers were found on bioreactor samples and cells were present on the internal surfaces of both static and bioreactor samples. The nuclei (blue) and F-actin (red) staining showed more uniform distribution in 20 rpm sample. White bar: 50 μm; yellow bar: 2.5 μm.

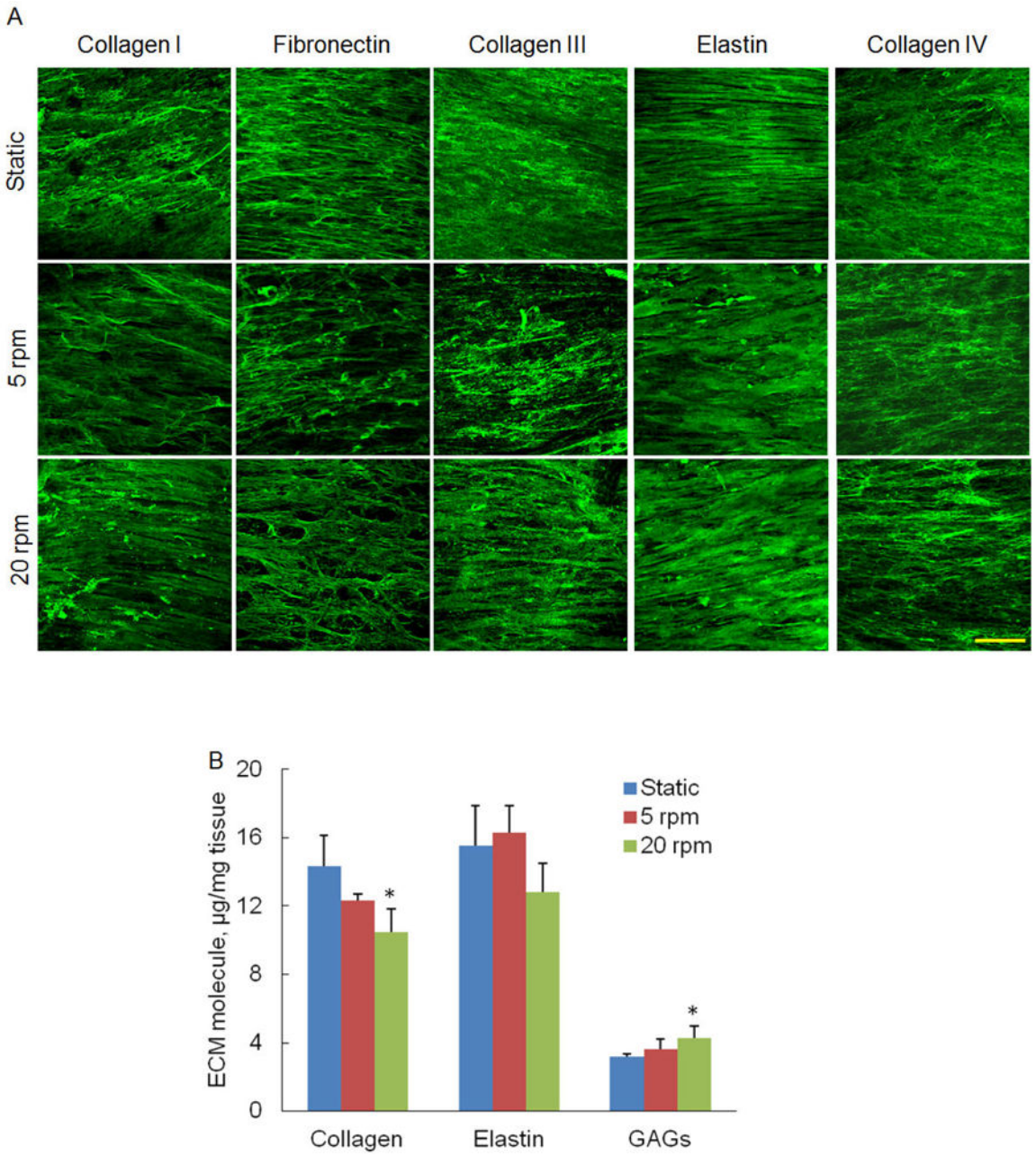

Figure 3.

Characterization of ECM proteins in the vascular grafts. (A) Immunofluorescence staining of ECM protein collagen I, fibronectin, collagen III, collagen IV and elastin in the wall of the construct. ECM fibers were aligned and thick fibers were observed on bioreactor samples. Scale bar: 50 μm. (B) ECM molecules content in the constructs including total collagen, elastin and GAGs. The collagen in 20 rpm sample significantly decreased and the GAGs in 20 rpm sample significantly increased. * $p < 0.05$ (compared to static sample).

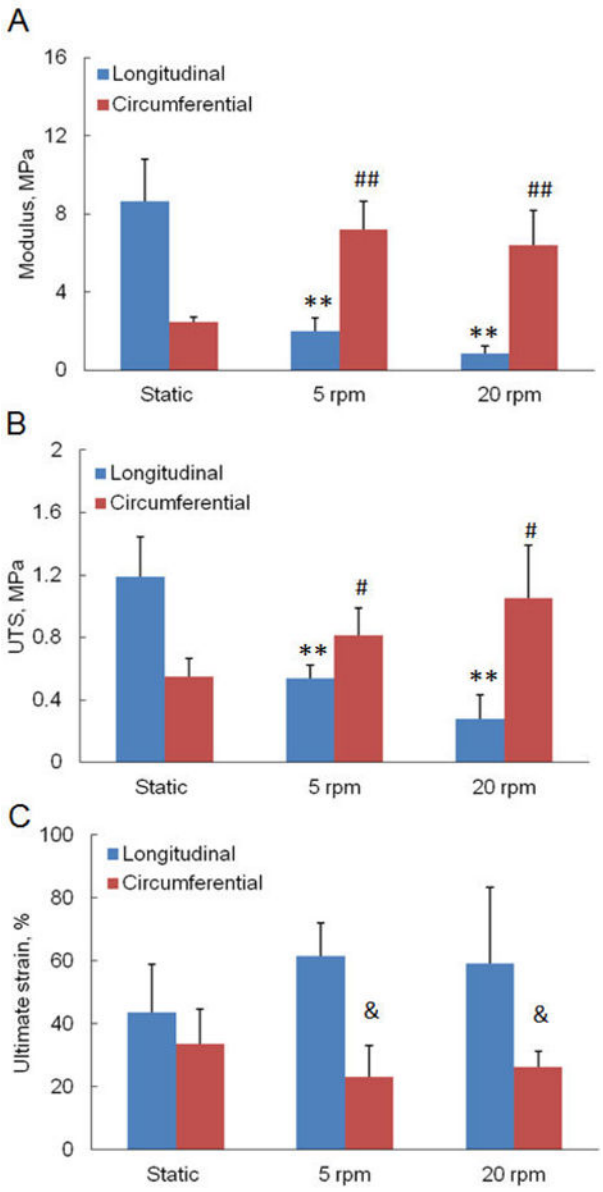

Figure 4.

Mechanical strength of the vascular grafts tested in longitudinal and circumferential directions. (A) elastic modulus; (B) ultimate tensile stress (UTS); (C) ultimate strain. All samples demonstrated anisotropic mechanical properties. Mechanical stress generated in the bioreactor improved the strength measured in circumferential direction but decreased the strength measured in longitudinal direction. * $p < 0.05$, ** $p < 0.01$ compared to longitudinal static samples; # $p < 0.05$, ## $p < 0.01$ compared to circumferential static samples; & $p < 0.05$ for comparison made between longitudinal and circumferential samples.

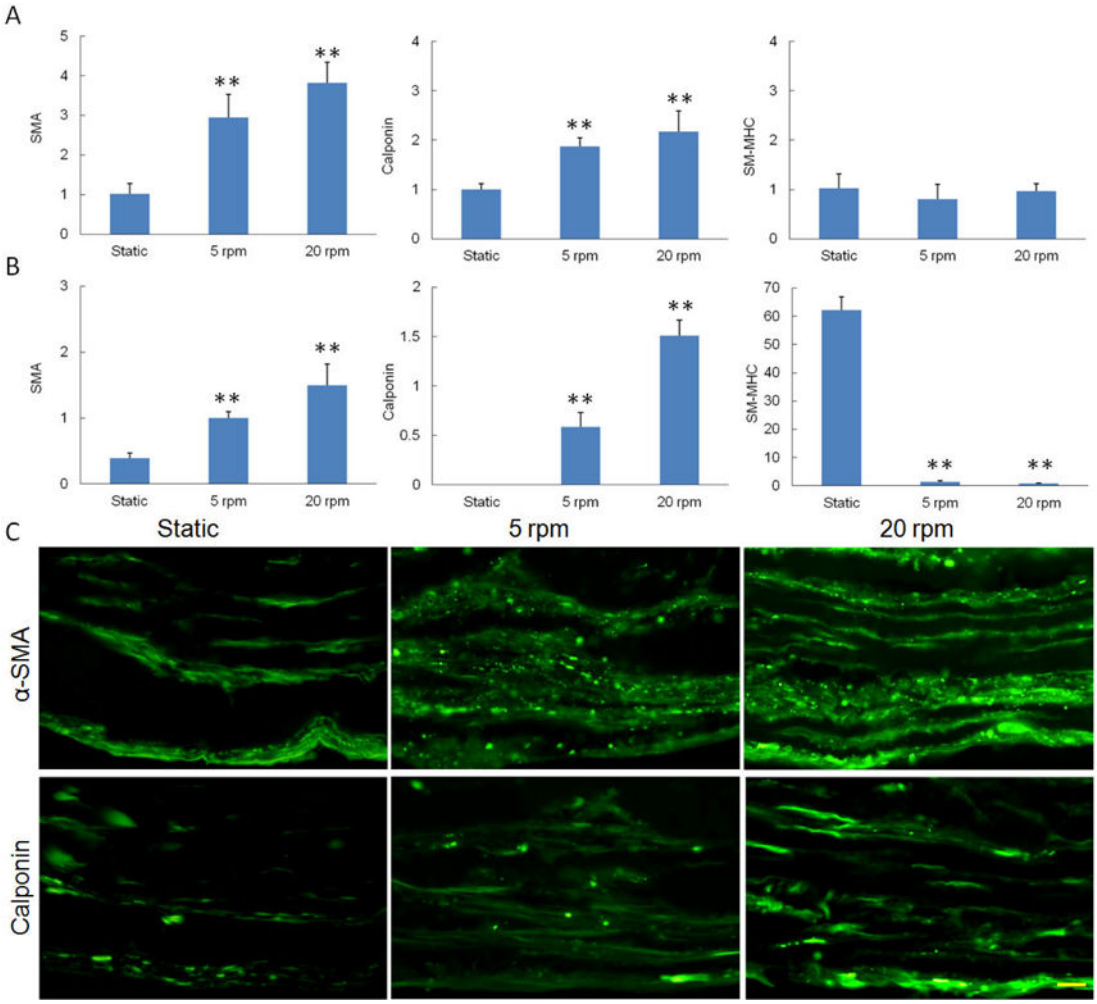

Figure 5.

Expression of smooth muscle cell (SMC) specific markers in the vascular grafts. (A) SMC specific genes expression of hMSC construct cultured in complete culture medium; (B) SMC specific genes expression of hMSC construct cultured in smooth muscle cell induction medium; (C) Immunofluorescent staining of SMC specific proteins in hMSC construct cultured in complete culture medium. ** $p < 0.01$ compared to static culture samples. Scale bar: 20 μm.